Received: 11 May 2023 | Revised: 26 June 2023 | Accepted: 27 June 2023

DOI: 10.1002/pro.4716

RESEARCH ARTICLE

THE PROTEIN SOCIETY WILEY

Trifluoroethanol and the behavior of a tardigrade desiccation-tolerance protein

Shikun Wang[1] | **Jonathan Eicher**[1] | **Gary J. Pielak**[1,2,3,4]

[1]Department of Chemistry, University of North Carolina at Chapel Hill, Chapel Hill, North Carolina, USA

[2]Department of Biochemistry & Biophysics, University of North Carolina at Chapel Hill, Chapel Hill, North Carolina, USA

[3]Lineberger Cancer Center, University of North Carolina at Chapel Hill, Chapel Hill, North Carolina, USA

[4]Integrative Program for Biological and Genome Sciences, University of North Carolina at Chapel Hill, Chapel Hill, North Carolina, USA

Correspondence
Gary J. Pielak, Department of Chemistry, University of North Carolina at Chapel Hill, Chapel Hill, NC, USA.
Email: gary_pielak@unc.edu

Funding information
National Institutes of Health; National Science Foundation

Review Editor: Aitziber L. Cortajarena

Abstract

The cosolvent 2,2,2-trifluoroethanol (TFE) is often used to mimic protein desiccation. We assessed the effects of TFE on cytosolic abundant heat soluble protein D (CAHS D) from tardigrades. CAHS D is a member of a unique protein class that is necessary and sufficient for tardigrades to survive desiccation. We find that the response of CAHS D to TFE depends on the concentration of both species. Dilute CAHS D remains soluble and, like most proteins exposed to TFE, gains α-helix. More concentrated solutions of CAHS D in TFE accumulate β-sheet, driving both gel formation and aggregation. At even higher TFE and CAHS D concentrations, samples phase separate without aggregation or increases in helix. Our observations show the importance of considering protein concentration when using TFE.

KEYWORDS

aggregation, desiccation tolerance, disorder, infrared spectroscopy, phase separation, tardigrades, trifluoroethanol

1 | INTRODUCTION

Protein-based drugs are prone to irreversible inactivation if not produced, transported, and stored at low temperature (Lagassé et al., 2017). Proteins dried with an excipient can be stable at higher temperatures, offering an alternative to the cold chain (Piszkiewicz & Pielak, 2019; Merivaara et al., 2021). To this end, cosolvents mimicking dehydration are used for probing protein protection. One such cosolvent, 2,2,2-trifluoroethanol (TFE), desolvates the polypeptide backbone by making water less hydrogen-bond competent, elevating the entropic cost of hydration (Kentsis & Sosnick, 1998; Anderson et al., 2010; Anderson & Webb, 2012). Although well-known for stimulating α-helix formation at higher percent volume/volume concentrations (%TFE), the cosolvent can induce β-sheet-driven aggregation at low-to-medium %TFE (Wei et al., 2006). TFE's possible dehydration-mimicking properties could thus be useful for understanding the mechanism of desiccation-tolerance proteins (Boothby & Pielak, 2017) and testing their potential as excipients. Studies of late embryogenesis abundant (LEA) proteins, which are desiccation-tolerance proteins found in plants and animals, report α-helix formation with increasing %TFE, without aggregation (Tolleter et al., 2007; Boswell et al., 2014; Hand & Menze, 2015).

Tardigrades, a phylum of microscopic animals that survive extreme environmental stresses, produce proteins that protect against desiccation stress (Yamaguchi et al., 2012; Boothby et al., 2017). These tardigrade-specific intrinsically disordered proteins (TDPs) form

helices in TFE, suggesting a hypothesis that helix formation leads to protection (Yamaguchi et al., 2012). However, the fact that TFE induces α-helix formation in most proteins lessens the veracity of this hypothesis and TFE's ability to mimic dehydration.

Here, we test this hypothesis by treating a potential biocompatible excipient, cytosolic abundant heat-soluble (CAHS) D, from tardigrades (Yamaguchi et al., 2012; Boothby et al., 2017; Piszkiewicz et al., 2019; Esterly et al., 2020; Crilly et al., 2022; Eicher et al., 2022) with TFE. We measured structural and phase changes by using circular dichroism spectropolarimetry (CD), ultraviolet–visible (UV–Vis) light scattering and attenuated total reflectance (ATR) Fourier transform infrared (FTIR)-spectroscopies. FTIR is useful because absorbances in the amide I region (1600–1700 cm^{-1}) can be related to secondary structure via analysis of spectra from known protein structures and the fitting of Voigt profiles (Barth, 2007).

CAHS D forms a thermo-reversible gel in vitro (Malki et al., 2021), which turns into an aerogel upon drying and these forms may serve as a shield to protect proteins from dehydration damage (Crilly et al., 2022; Eicher et al., 2023). Thus, investigating the physical and structural response of CAHS D to TFE may not only clarify TFE's role in mimicking desiccation but it may also provide clues about the protective mechanism used by the tardigrade protein.

2 | RESULTS

2.1 | α-Helix at low cytosolic abundant heat soluble protein D concentration in 2,2,2-trifluoroethanol

We acquired solution CD spectra (Figure 1a, b) as a function of CAHS D and TFE concentrations. At low CAHS D concentration (0.2 g/L), in the absence of TFE, the protein exhibits a single negative Cotton effect around 200 nm, indicative of disorder (Figure 1a) (Chemes et al., 2012). The amount of α-helix, as indicated by the appearance of minima at 206 and 220 nm, increases with %TFE. Similar results are observed for other desiccation-tolerance proteins (Yamaguchi et al., 2012). Quantification of the spectra corroborates these observations and shows the formation of parallel β-sheets at low %TFE (Figure 1c). Sheets never predominate and decrease greatly above 30% TFE.

Increasing the CAHS D concentration to 0.4 g/L (Figure 1b) alters the response. Characteristic α-helical features are still observed at 50% and 70% TFE, consistent with the expectation that TFE induces helices. But unlike what is observed at low CAHS D concentrations, the helices do not arise directly from random coils. Instead, the protein loses its coil-like spectrum and gains β-character at both 10% and 25% TFE, as indicated by the negative Cotton effect near 230 nm, similar to the spectrum of the

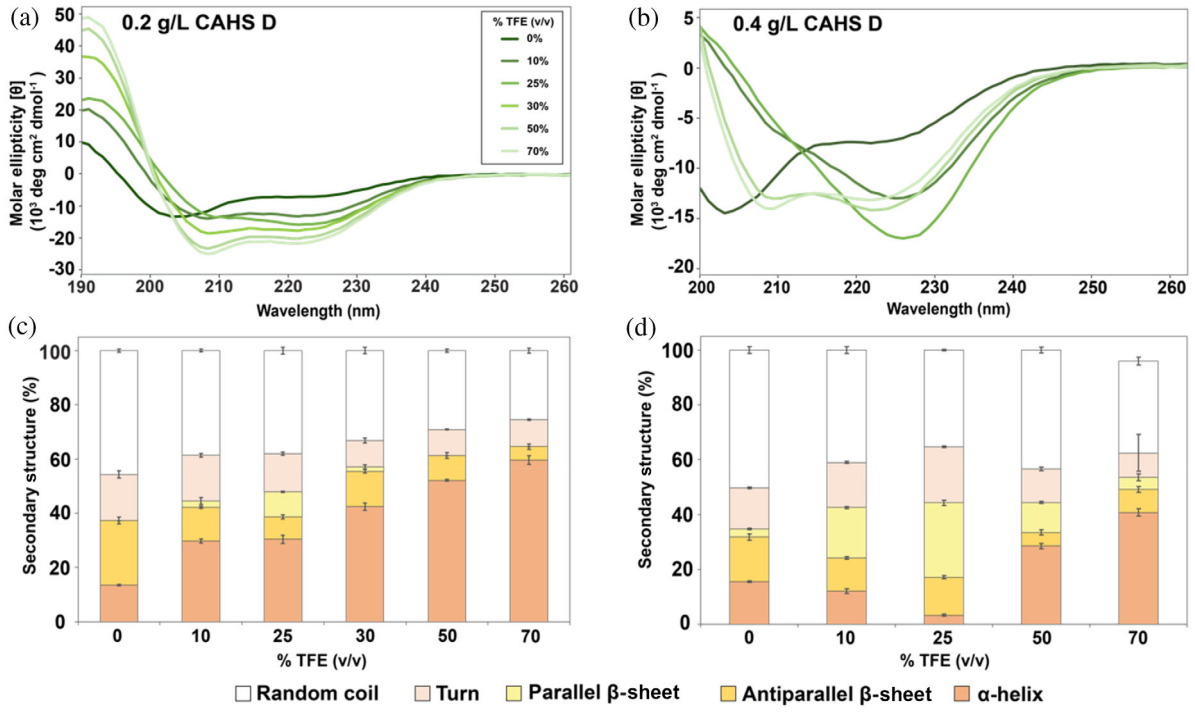

FIGURE 1 TFE effects at low cytosolic abundant heat soluble protein D (CAHS D) concentration. Solution CD spectra with increasing %TFE at 0.2 g/L (a) and 0.4 g/L CAHS D (b). Secondary structure at 0.2 g/L (c) and 0.4 g/L (d) CAHS D. Bars are presented as the mean with the standard deviation from three independent samples.

all β-protein, concanavalin A (Sen et al., 2009). Quantitative analysis supports this conclusion (Figure 1d). Thus, increasing the CAHS concentration, which increases the potential for intermolecular interactions causes TFE to first promote β-sheet formation, which then converts to α-helix at higher TFE concentrations.

We observed that at even higher CAHS D concentrations (0.5–1.4 g/L) CAHS D samples become viscous gels in 10% TFE, show aggregates at 25% TFE, and return to a single-phase liquid at 50% TFE. Due to the high protein concentration, the secondary structure could not be assessed by CD because of the unacceptably large far-UV absorbance even in our shortest pathlength cuvette. Aggregation was quantified by measuring scattered light at 405 nm at 0.2, 0.4, and 1.4 g/L CAHS D in TFE. Maximum scattering occurs at 25% TFE at the highest CAHS concentration but decreases sharply at 50% v/v TFE (Figure 2).

2.2 | β-Sheet, not α-helix, contributes to 2,2,2-trifluoroethanol-induced gelation

Phase separation is observed with increasing %TFE at higher CAHS D concentrations of 5.0–20 g/L (Figure 3). At 20 g/L, increasing the TFE concentration causes CAHS D samples to progress from a gel phase through a gel-plus-aggregate phase to liquid-gel phase separation. As the concentration of CAHS D increases, the amount of TFE required for the phase separation decreases.

The secondary structure of CAHS D in the phase transition was quantified by fitting the amide I region of FTIR spectra. Reliable spectra could only be obtained at 20 g/L CAHS D because the signal to noise ratio was too low at 5 and 10 g/L. The proportion of α-helices is independent of TFE, ranging from 40% to 50% (Figure S1), and the change is insignificant compared to data for other desiccation-tolerance proteins, which gain much more helix (Tolleter et al., 2007).

To investigate the nature of the TFE-induced gel, melting points (T_m values, Figure 4) were measured using FTIR by acquiring spectra from 303 to 318 K (Figure S2). At 30 g/L CAHS D, T_m increases from 303.3 ± 0.9 K at 0% TFE to 310.2 ± 0.3 K at 5% TFE, which is similar to the T_m observed for 50 g/L CAHS D at 0% TFE (310 ± 2 K). At 303.5 K, there is an insignificant change in

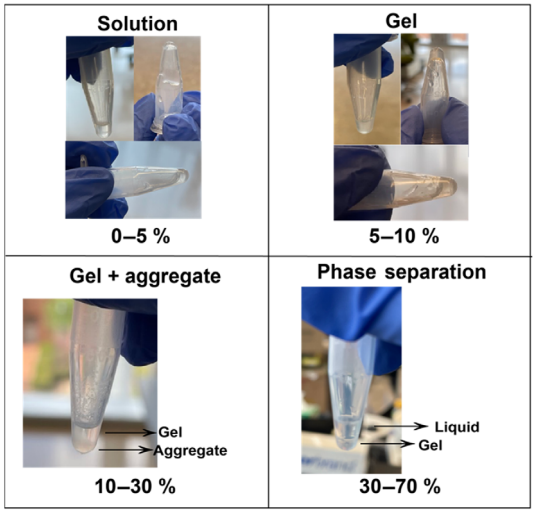

FIGURE 3 Behavior of 20 g/L cytosolic abundant heat soluble protein D (CAHS D) in 2,2,2-trifluoroethanol (TFE). The properties were similar for CAHS D from 5 to 20 g/L.

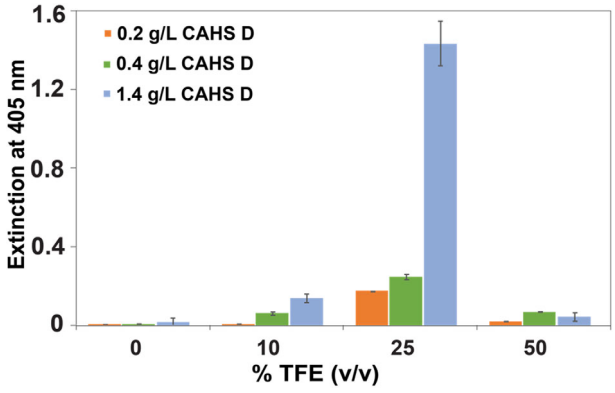

FIGURE 2 Optically monitored aggregation of cytosolic abundant heat soluble protein D (CAHS D) in TFE. TFE increases aggregation up to a concentration of 25%. Data are presented as the mean and standard deviation from three independent samples.

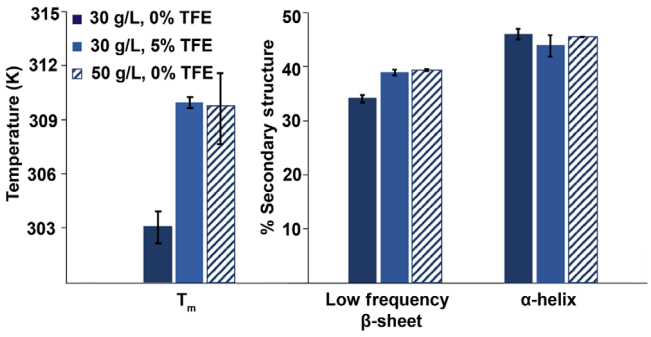

FIGURE 4 TFE effects on T_m and % secondary structure (303.5 K) at high (30 g/L) cytosolic abundant heat soluble protein D (CAHS D) concentration. Low frequency β-sheet increases with T_m (from the Gibbs-Helmholtz equation). Data reported as mean ± standard deviation from three independent samples. Tukey's range test shows a significant difference ($p < 0.002$) in T_m between 30 g/L CAHS/0% TFE and the other values and shows a highly significant difference ($p < 0.0007$) in β-sheet content between 30 g/L CAHS/0% TFE and other values. Other differences are not significant.

α-helix with increasing TFE, but the amount of low frequency β-sheet increases slightly with TFE and CAHS D concentration (Figure 4). Thus, TFE increases the strength of the gel, probably by increasing the amount of intermolecular β-sheet.

2.3 | Cytosolic abundant heat soluble protein D gels do not form aggregates at high %TFE

FTIR was used to characterize liquid-gel phase separation in 20 g/L CAHS D at high %TFE. Compared to gel spectra, which generally show high absorbance in the amide I and II regions (1500–1800 cm^{-1}), spectra of the liquid phase exhibit lower absorbances without an amide II peak (Figure S3a). Thus, CAHS D accumulates in the gel phase. Meanwhile, the liquid phase has a larger absorbance in the region characteristic of TFE (1000–1400 cm^{-1}) than does the gel phase (Figure S3b). In summary, the protein-rich gel phase is TFE poor, and the protein poor liquid phase is TFE rich.

To estimate %TFE in the protein-rich phase ($\%TFE_r$), the ratio of TFE peak area in the protein-rich phase (A_r) to the area in buffer (A_B) is multiplied by the value from buffer samples of standardized %TFE ($\%TFE_B$).

$$\%TFE_r = \%TFE_B * \left(\frac{A_r}{A_B}\right) \quad (1)$$

In the presence of phase separation, no matter how much TFE is used to prepare the sample, the protein-rich phase contains 26.8% ± 0.9% TFE, which is approximately the %TFE at the transition from gel plus aggregates to liquid-gel phase separation (Figure 5).

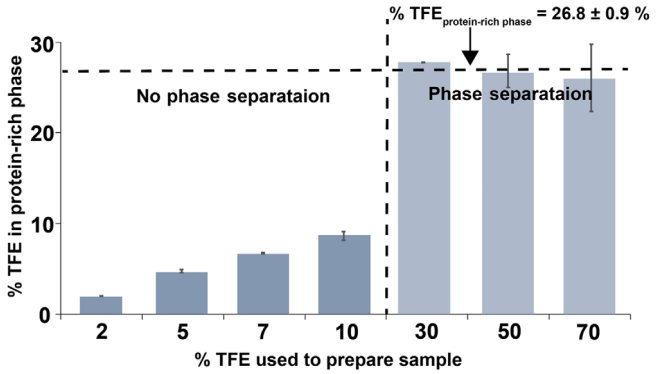

FIGURE 5 %TFE in a 20 g/L sample of cytosolic abundant heat soluble protein D (CAHS D) with and without phase separation. Below 30% TFE there is no separation. At ≥30% a protein poor and a protein rich phase are observed. %TFE in the rich phase is 26.8 ± 0.9% regardless of the amount of TFE used to prepare the sample. Data reported as mean ± standard deviation from three independent samples.

3 | DISCUSSION

We investigated the effects of the desolvating agent TFE on CAHS D. At 0.2 and 0.4 g/L CAHS D neither gelation nor aggregation is observed on adding TFE. At both protein concentrations, CD data indicate a shift to α-helix from random coil with increasing %TFE (Figure 1). At 0.4 g/L, CAHS D shows a more significant increase in parallel β-sheets between 10% and 30% TFE than it does at 0.2 g/L, indicating the potential of TFE to induce β-sheets.

Other reports on disordered desiccation-tolerance proteins in TFE report only helix formation. Those results, which were acquired at low protein concentration were interpreted as showing a relationship between α-helix formation and dehydration (Tolleter et al., 2007; Boswell et al., 2014; Hand & Menze, 2015; Yamaguchi et al., 2012). However, TFE stabilizes helical structures in most proteins, whether folded or disordered (Anderson et al., 2010; Anderson & Webb, 2012; Wei et al., 2006; Ataei & Hosseinkhani, 2015; Srisailam et al., 2002). We therefore sought additional information by using higher CAHS D concentrations.

CAHS D forms a hydrogel, which has been related to its desiccation tolerance (Malki et al., 2021). In the absence of TFE, gelation becomes evident at concentrations >20 g/L. However, at 1.4 g/L CAHS D and moderate TFE concentrations, both gel and aggregate are present, as indicated by the light scattering data and the mechanical properties of the samples (Figures 2 and 3).

Upon increasing %TFE, the gel is replaced by aggregates, which then disappear at yet higher %TFE. At lower CAHS D concentrations (0.2 and 0.4 g/L), aggregates are absent, and only small amounts of parallel β-sheets (Figure 1c, d) are observed. These findings are consistent with studies of aggregates related to Alzheimer's and prion diseases where aggregation increases with increasing parallel β-sheet content (Benzinger et al., 1998; Chan et al., 2005). Studies of proteins unrelated to desiccation tolerance also report aggregation at low-to-medium % TFE, suggesting that aggregation arises from the formation of non-native, fibrillar intermolecular β-sheets in these proteins (Anderson et al., 2010; Anderson & Webb, 2012; Srisailam et al., 2002) We are unable to quantify the secondary structure of 1.4 g/L CAHS D because the concentration is too low for FTIR but too high for CD in this combination of gel and aggregates. We suggest, however, that the structure comprises intermolecular parallel β-sheets, whose content increases with

increasing protein concentration. Other studies of desiccation-tolerance proteins do not report gelation or aggregation, probably because the protein concentration was low, leading to sparse intermolecular interactions. We suggest that the disappearance of aggregates at higher %TFE corresponds to the weakening of β-sheets and the strengthening of α-helices (Eicher et al., 2022).

Further increases in CAHS D concentration (5–20 g/L) result in more significant gel and aggregate formation at low-to-medium %TFE (Figure 3). Quantification of secondary structure does not show a shift towards α-helix with increasing %TFE, suggesting TFE-induced gelation and aggregation are not directly linked to helix formation (Figure S1). Melting curves show that T_m increases with increasing %TFE (Figure S2). Knowing that T_m is also positively correlated with protein concentration (Eicher et al., 2022), we suggest that increasing CAHS D concentration contributes to the formation of intermolecular β-sheets, leading to stronger gels. FTIR data support this hypothesis, showing a significant increase in low frequency β-sheets in TFE (Figure 4). Low frequency β-sheets are more ordered and tend to form intermolecular interactions (Lomont et al., 2017; Baird et al., 2020). Thus, at low-to-medium %TFE, increasing TFE concentration is likely to strengthen the interactions between intermolecular β-sheets, turning CAHS D from liquid to gel to aggregates.

More concentrated CAHS D (5–20 g/L) phase separates at 30%–70 %TFE (Figure 3). Phase separation has been reported for other desiccation tolerance (Tanaka et al., 2022) and other proteins (Hattori et al., 2018; Dyksterhuis et al., 2007) and when TFE is used to extract and purify membrane proteins (Koolivand et al., 2018; Deshusses et al., 2003). Analysis of the two phases reveals a protein-rich TFE-poor gel phase and a protein-poor TFE-rich liquid phase (Figure S3). Quantification (Figure 5) shows that above 30% TFE, instead of further aggregation or a shift to helices, CAHS D gels maintain an average of 26.8% ± 0.9% TFE, forcing any additional TFE into the protein-poor phase. This observation suggests that CAHS D hydrogels are capable of partitioning small molecules based on bulk properties, for example, hydrophobicity.

In summary, TFE-induced changes in CAHS D depend on protein concentration (Figure 6). In dilute CAHS D (<5 g/L), the protein forms weak intermolecular β-sheet interactions. Thus, although parallel β-sheets are induced at low-to-medium %TFE at CAHS D concentrations as low as 0.2 g/L, gelation and aggregation are not observed until the protein concentration exceeds 1.4 g/L. At >30% TFE, preferential TFE-protein solvation favors helices rather than intermolecular β-sheets, leading to the disappearance of aggregation, in contrast to the lyophilized samples (Eicher et al., 2023).

Aggregation or helix formation is not unique to desiccation-tolerance proteins but TFE-induced gelation, as is observed for CAHS D, may be key to the role of this protein in desiccation protection. Replacement of the gel

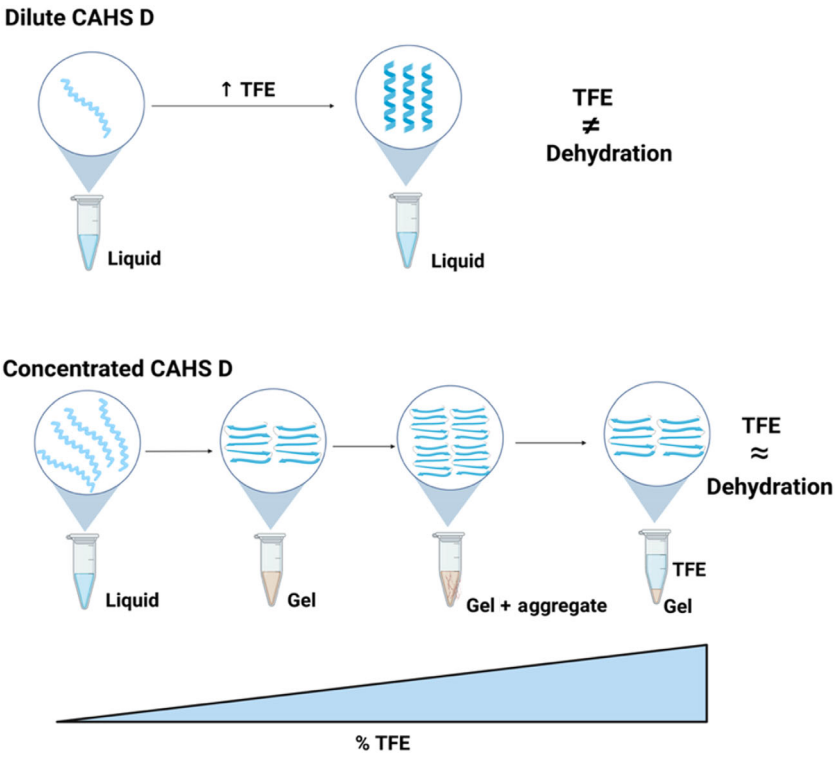

FIGURE 6 Dilute and concentrated CAHS D structure and phase behavior with increasing %TFE (Created with Biorender).

by aggregates and helices suggests that TFE might be a poor mimic of dehydration, at least for dilute CAHS D. When CAHS D concentration is too low to form intermolecular sheets, there is no gelation, and TFE shifts CAHS D to α-helix, as TFE does for most proteins.

When CAHS D is more concentrated, TFE-induced intermolecular interactions between ordered low frequency β-sheets drive gelation (Figure 6) (Eicher et al., 2022). As %TFE increases, β-sheets interactions grow stronger, leading to aggregation. At high %TFE (>30%), the CAHS D samples spontaneously phase separate, forming a gel that rejects further aggregation or structural rearrangement.

We can also compare the secondary structure in TFE to the secondary structure of lyophilized CAHS D. At low concentrations (0.1–10 g/L) there is little change upon drying (Eicher et al., 2023), which contrasts with what happens in TFE solution as assessed by using CD (Figure 1). In addition, the secondary structure as assessed by FTIR (Figure 4) is not comparable to the secondary structure of lyophilized samples (Eicher et al., 2023) and drying CAHS D from higher concentration solutions result in less, not more, α-helix (Eicher et al., 2023).

In summary, at low protein concentration TFE enhances the helix content for almost all proteins, including CAHS D. At intermediate CAHS D concentrations, the desolvating properties of TFE favor β-sheet but further increases in TFE force α-helix formation, which inhibits gelation. Further increases in CAHS concentration lead to formation of intermolecular β-sheets (Eicher et al., 2022) and the desolvating properties of TFE stabilize the sheets resulting in protein aggregation and the formation of stronger gels. At the highest concentrations of CAHS D, TFE causes separation into two phases—a protein-poor, TFE-rich phase and a gel-like protein-rich, TFE-poor phase. Thus, it too simple to consider TFE a mimic of dehydration.

4 | MATERIALS AND METHODS

4.1 | Cytosolic abundant heat soluble protein D

CAHS D was prepared as described (Esterly et al., 2020). Briefly, a pET28-b plasmid containing the his-tagged structural gene for CAHS D was transformed into BL21 (DE3) *E. coli* cells. The cells were grown in Lennox broth, and protein expression was induced with isopropyl β-D-1-thiogalactopyranoside. The cells were harvested lysed by heat shock, and the lysate cleared by centrifugation. The supernatant was diluted with an equal volume of urea-containing buffer, loaded onto a His-Trap HP column (Thermo Fisher, Waltham, MA) and eluted with a gradient of imidazole-urea buffer. Sodium dodecyl sulfate–polyacrylamide gel electrophoresis (SDS-PAGE) was used to identify fractions containing CAHS D. The his tag was removed with tobacco etch virus protease. Fractions containing only CAHS D were combined, lyophilized, and resuspended in physiologically buffered saline (PBS, 140 mM NaCl, 2.7 mM KCl, 8 mM Na_2HPO_4 pH 7.4). CAHS D concentration was quantified with a Pierce Coomassie Plus assay (Bradford, 1976) using bovine serum albumin (Thermo Fisher) as the standard. For studying the effects of drying, lyophilized samples were resuspended in water, the concentration quantified as described above, and the sample diluted to the appropriate target concentration before lyophilization.

4.2 | UV–Vis

Aggregation of CAHS D was quantified with a UV–Vis SmartSpec Plus spectrophotometer (BioRad, Hercules, CA) by measuring the absorbance at 405 nm in a 1-cm quartz cuvette (Hellma, Plainville, NY). TFE was mixed with PBS before addition. The incubation time was 30 min. Aggregation was estimated by subtracting the absorbance of the buffer (PBS) blank (Ataei & Hosseinkhani, 2015; Srisailam et al., 2002).

4.3 | CD

Spectra were obtained at CAHS D concentrations of <2 g/L from 280 to 185 nm using a Chirascan™-Plus (Applied Photophysics, Leatherland, UK) spectropolarimeter at 30°C. Phosphate buffer (10 mM, 6.1 mM Na_2HPO_4, 3.9 mM NaH_2PO4, pH 7.4) was used instead of PBS to minimize interference from Cl^-. TFE was mixed with buffer before adding it to the sample. The samples were incubated for 30 min and spectra acquired in a 1-mm quartz cuvette (Hellma). The results are reported in molar ellipticity, $[\theta] = \frac{m^\circ * M}{10 * L * c}$ in units of degree $cm^2/dmol$, where c is the concentration of protein in g/L, L is the cuvette pathlength in cm, and M is the mean residue weight of the protein (112.27 g/mol) (Purdie, 1996). Secondary structure was estimated using Beta Structure Selection (BEStSel) software (Micsonai et al., 2015).

4.3.1 | FTIR

Spectra (400 scans) were acquired at concentrations >5 g/L CAHS D using a Prota-3S FT-IR Spectrophotometer (BioTools, Jupiter FL) at 30°C, with a resolution of 4 cm^{-1}. TFE was either added last or mixed with PBS before dilution, followed by a 30 min incubation. Background-,

buffer-, and sample- spectra were preprocessed using Prota3s (BioTools) software. Background spectra were subtracted from both buffer- and sample spectra. Buffer spectra were then subtracted from sample spectra in the same proportion in each sample. Optimal subtraction was accomplished by ensuring that the final spectra are non-negative near 3750 cm^{-1} and flat between 1800 and 2000 cm^{-1}. Processed spectra were loaded onto the Orange Data Mining platform (Demšar et al., 2013), smoothed with a Savitsky-Golay filter (window of 5) and denoised via principal component analysis (PCA) (4 components). Smoothed bands were processed with a positive rubber band baseline-correction, vector normalized, and fitted with Voigt profiles using non-linear least-squares regression. Secondary structures were assigned as described (Demšar et al., 2013). We used the ATR crystal to take 100 scans of lyophilized samples, subtracting an appropriate background followed by the processing steps described above. For the temperature studies (30–50°C), the scan number was 100. PCA was applied to the smoothed spectra. Melting curves were obtained by plotting the first component, which explains the largest variation, against temperature. Data were fitted to the two-state Gibbs-Helmholtz equation using Matlab to obtain the midpoint temperature, T_m (Cohen & Pielak, 1994). The integrated areas under the TFE absorbances were used to obtain %TFE.

AUTHOR CONTRIBUTIONS

Shikun Wang, Jonathan Eicher, and Gary J. Pielak designed research, Shikun Wang and Jonathan Eicher performed research, Shikun Wang, Jonathan Eicher, and Gary J. Pielak analyzed data; and Shikun Wang, Jonathan Eicher, and Gary J. Pielak wrote the paper.

ACKNOWLEDGMENTS

This work was supported by the National Science Foundation (CHE-2203505) and the National Institutes of Health (R01GM127291). We thank the Pielak lab for helpful discussions, Elizabeth Pielak for comments on the manuscript, Ashutosh Tripathy of the Macromolecular Interactions Facility (NIH P30CA016086) for assistance with CD, and Rafael F. Irgolič for automating spectra collection. SW was awarded the UNC Chemistry Venable Medal for this project.

CONFLICT OF INTEREST STATEMENT

The authors declare no conflicts of interest.

ORCID

Shikun Wang https://orcid.org/0009-0003-9628-2785
Jonathan Eicher https://orcid.org/0000-0002-2631-3385
Gary J. Pielak https://orcid.org/0000-0001-6307-542X

REFERENCES

Anderson V, Webb W. A desolvation model for trifluoroethanol-induced aggregation of enhanced green fluorescent protein. Biophys J. 2012;102:897–906.

Anderson VL, Ramlall TF, Rospigliosi CC, Webb WW, Eliezer D. Identification of a helical intermediate in trifluoroethanol-induced α-synuclein aggregation. Proc Natl Acad Sci U S A. 2010;107:18850–5.

Ataei F, Hosseinkhani S. Impact of trifluoroethanol-induced structural changes on luciferase cleavage sites. J Photochem Photobiol B. 2015;144:1–7.

Baird G, Farrell C, Cheung J, Semple A, Blue J, Ahl PL. FTIR spectroscopy detects intermolecular β-sheet formation above the high temperature T_m for two monoclonal antibodies. Protein J. 2020;39:318–27.

Barth A. Infrared spectroscopy of proteins. Biochim Biophys Acta. 2007;1767:1073–101.

Benzinger TLS, Gregory DM, Burkoth TS, Miller-Auer H, Lynn DG, Botto RE, et al. Propagating structure of Alzheimer's β-amyloid (10–35) is parallel β-sheet with residues in exact register. Proc Natl Acad Sci U S A. 1998;95:13407–12.

Boothby TC, Pielak GJ. Intrinsically disordered proteins and desiccation tolerance: elucidating functional and mechanistic underpinnings of anhydrobiosis. Bioessays. 2017;39:1700119.

Boothby TC, Tapia H, Brozena AH, Piszkiewicz S, Smith AE, Giovannini I, et al. Tardigrades use intrinsically disordered proteins to survive desiccation. Mol Cell. 2017;65:975–84.

Boswell LC, Menze MA, Hand SC. Group 3 late embryogenesis abundant proteins from embryos of *Artemia franciscana*: structural properties and protective abilities during desiccation. Physiol Biochem Zool. 2014;87:640–51.

Bradford MM. A rapid and sensitive method for the quantitation of microgram quantities of protein utilizing the principle of protein dye binding. Anal Biochem. 1976;72:248–54.

Chan JCC, Oyler NA, Yau W-M, Tycko R. Parallel β-sheets and polar zippers in amyloid fibrils formed by residues 10–39 of the yeast prion protein Ure2p. Biochemistry. 2005;44:10669–80.

Chemes LB, Alonso LG, Noval MG, de Prat-Gay G. Circular dichroism techniques for the analysis of intrinsically disordered proteins and domains. Methods Mol Biol. 2012;895:387–404.

Cohen DS, Pielak GJ. Stability of yeast iso-1-cytochrome *c* as a function of pH and temperature. Protein Sci. 1994;3:1253–60.

Crilly CJ, Brom JA, Warmuth O, Esterly HJ, Pielak GJ. Protection by desiccation-tolerance proteins probed at the residue level. Protein Sci. 2022;31:396–406.

Demšar J, Curk T, Erjavec A, Gorup Č, Hočevar T, Milutinovič M, et al. Orange: data mining toolbox in Python. J Mach Learn Res. 2013;14:2349–53.

Deshusses JMP, Burgess JA, Scherl A, Wenger Y, Walter N, Converset V, et al. Exploitation of specific properties of trifluoroethanol for extraction and separation of membrane proteins. Proteomics. 2003;3:1418–24.

Dyksterhuis LB, Baldock C, Lammie D, Wess TJ, Weiss AS. Domains 17–27 of tropoelastin contain key regions of contact for coacervation and contain an unusual turn-containing cross-linking domain. Matrix Biol. 2007;26:125–35.

Eicher JE, Brom JA, Wang S, Sheiko SS, Atkin JM, Pielak GJ. Secondary structure and stability of a gel-forming tardigrade desiccation-tolerance protein. Protein Sci. 2022;31:e4495.

Eicher JE, Hutcheson BO, Pielak GJ. Properties of a tardigrade desiccation-tolerance protein aerogel. Biophys J. 2023;122:2500–5.

Esterly HJ, Crilly CJ, Piszkiewicz S, Shovlin DJ, Pielak GJ, Christian BE. Toxicity and immunogenicity of a tardigrade cytosolic abundant heat soluble protein in mice. Front Pharmacol. 2020;11:565969.

Hand SC, Menze MA. Molecular approaches for improving desiccation tolerance: insights from the brine shrimp *Artemia franciscana*. Planta. 2015;242:379–88.

Hattori T, Itagaki T, Uji H, Kimura S. Temperature-induced phase separation in molecular assembly of nanotubes comprising amphiphilic polypeptoid with poly(N-ethyl glycine) in water by a hydrophilic-region-driven-type mechanism. J Phys Chem B. 2018;122:7178–84.

Kentsis A, Sosnick TR. Trifluoroethanol promotes helix formation by destabilizing backbone exposure: Desolvation rather than native hydrogen bonding defines the kinetic pathway of dimeric coiled coil folding. Biochemistry. 1998;37:14613–22.

Koolivand A, Clayton S, Rion H, Oloumi A, O'Brien A, Khaledi MG. Fluoroalcohol-induced coacervates for selective enrichment and extraction of hydrophobic proteins. J Chromatogr B Biomed Sci Appl. 2018;1083:180–8.

Lagassé HAD, Alexaki A, Simhadri VL, Katagiri NH, Jankowski W, Sauna ZE, et al. Recent advances in (therapeutic protein) drug development. Drug Dev. 2017;6:113.

Lomont JP, Ostrander JS, Ho J-J, Petti MK, Zanni MT. Not all β-sheets are the same: amyloid infrared spectra, transition dipole strengths, and couplings investigated by 2D IR spectroscopy. J Phys Chem B. 2017;121:8935–45.

Malki A, Teulon J-M, Camacho Zarco A, Chen S-wW, Adamski W, Maurin D, et al. Intrinsically disordered tardigrade proteins self-assemble into fibrous gels in response to environmental stress. Angew Chem Int Ed. 2021;61:e202109961.

Merivaara A, Zini J, Koivunotko E, Valkonen S, Korhonen O, Fernandes FM, et al. Preservation of biomaterials and cells by freeze-drying: change of paradigm. J Control Release. 2021;336:480–98.

Micsonai A, Wien F, Kernya L, Lee Y-H, Goto Y, Réfrégiers M, et al. Accurate secondary structure prediction and fold recognition for circular dichroism spectroscopy. Proc Natl Acad Sci U S A. 2015;112:E3095–103.

Piszkiewicz S, Pielak G. Protecting enzymes from stress-induced inactivation. Biochemistry. 2019;58:3825–33.

Piszkiewicz S, Gunn KH, Warmuth O, Propst A, Mehta A, Nguyen KH, et al. Protecting activity of desiccated enzymes. Protein Sci. 2019;28:941–51.

Purdie N. Circular dichroism and the conformational analysis of biomolecules. New York: Plenum Press; 1996. p. 738.

Sen P, Fatima S, Khan JM, Khan RH. How methyl cyanide induces aggregation in all-alpha proteins: a case study in four albumins. Int J Biol Macromol. 2009;44:163–9.

Srisailam S, Kumar TKS, Srimathi T, Yu C. Influenceof backbone conformation on protein aggregation. J Am Chem Soc. 2002;124:1884–8.

Tanaka A, Nakano T, Watanabe K, Masuda K, Honda G, Kamata S, et al. Stress-dependent cell stiffening by tardigrade tolerance proteins that reversibly form a filamentous network and gel. PLoS Biol. 2022;20:e3001780.

Tolleter D, Jaquinod M, Mangavel C, Passirani C, Saulnier P, Manon S, et al. Structure and function of a mitochondrial late embryogenesis abundant protein are revealed by desiccation. Plant Cell. 2007;19:1580–9.

Wei X, Ding S, Jiang Y, Zeng X-G, Zhou H-M. Conformational changes and inactivation of bovine carbonic anhydrase II in 2,2,2-trifluoroethanol solutions. Biochemistry (Moscow). 2006;71:S77–82.

Yamaguchi A, Tanaka S, Yamaguchi S, Kuwahara H, Takamura C, Imajoh-Ohmi S, et al. Two novel heat-soluble protein families abundantly expressed in an anhydrobiotic tardigrade. PloS One. 2012;7:e44209.

SUPPORTING INFORMATION

Additional supporting information can be found online in the Supporting Information section at the end of this article.

How to cite this article: Wang S, Eicher J, Pielak GJ. Trifluoroethanol and the behavior of a tardigrade desiccation-tolerance protein. Protein Science. 2023;32(8):e4716. https://doi.org/10.1002/pro.4716